Cell Metabolism
Article

Rcf1 Mediates Cytochrome Oxidase Assembly and Respirasome Formation, Revealing Heterogeneity of the Enzyme Complex

Milena Vukotic,[1,4] Silke Oeljeklaus,[5,7] Sebastian Wiese,[5,7] F. Nora Vögtle,[4] Chris Meisinger,[4,7] Helmut E. Meyer,[8] Anke Zieseniss,[2] Doerthe M. Katschinski,[2] Daniel C. Jans,[9] Stefan Jakobs,[3,9] Bettina Warscheid,[5,6,7] Peter Rehling,[1,10,*] and Markus Deckers[1]

[1]Department of Biochemistry II
[2]Department of Cardiovascular Physiology
[3]Department of Neurology
University of Göttingen, D-37073 Göttingen, Germany
[4]Institute for Biochemistry and Molecular Biology, Center for Biochemistry and Molecular Cell Science
[5]Institute for Biology II, Faculty for Biologie, Functional Proteomics
[6]Center for Biological Systems Analysis
[7]BIOSS Centre for Biological Signalling Studies
University of Freiburg, D-79104 Freiburg, Germany
[8]Medizinisches Proteom-Center, Ruhr-University Bochum, D-44801 Bochum, Germany
[9]Department of NanoBiophotonics, Mitochondrial Structure and Dynamics Group, Max-Planck Institute for Biophysical Chemistry, D-37077 Göttingen, Germany
[10]Max-Planck Institute for Biophysical Chemistry, D-37077, Göttingen, Germany
*Correspondence: peter.rehling@medizin.uni-goettingen.de
DOI 10.1016/j.cmet.2012.01.016

SUMMARY

The terminal enzyme of the mitochondrial respiratory chain, cytochrome oxidase, transfers electrons to molecular oxygen, generating water. Within the inner mitochondrial membrane, cytochrome oxidase assembles into supercomplexes, together with other respiratory chain complexes, forming so-called respirasomes. Little is known about how these higher oligomeric structures are attained. Here we report on Rcf1 and Rcf2 as cytochrome oxidase subunits in *S. cerevisiae*. While Rcf2 is specific to yeast, Rcf1 is a conserved subunit with two human orthologs, RCF1a and RCF1b. Rcf1 is required for growth in hypoxia and complex assembly of subunits Cox13 and Rcf2, as well as for the oligomerization of a subclass of cytochrome oxidase complexes into respirasomes. Our analyses reveal that the cytochrome oxidase of mitochondria displays intrinsic heterogeneity with regard to its subunit composition and that distinct forms of respirasomes can be formed by complex variants.

INTRODUCTION

The majority of cellular ATP is generated by oxidative phosphorylation within mitochondria. In this process, the respiratory chain establishes a proton gradient across the inner membrane of mitochondria that drives the F_1F_oATPase to generate ATP from ADP and anorganic phosphate, which is subsequently transported out of mitochondria by the ADP/ATP carrier. The cytochrome oxidase (complex IV) is the terminal enzyme of the respiratory chain. It receives electrons from cytochrome *c*, transports two protons across the inner membrane, and reduces molecular oxygen to water (Saraste, 1999; Tsukihara et al., 1996; Yoshikawa et al., 2011). The cytochrome oxidase is functionally highly conserved from bacteria to man but acquired increased complexity with regard to its composition throughout evolution. In human mitochondria it is comprised of three mitochondria-encoded membrane proteins (Cox1, Cox2, and Cox3) that assemble with ten nuclear-encoded proteins into an intricate membrane-embedded entity in a process that requires numerous specific assembly factors (Carr and Winge, 2003; Fontanesi et al., 2008; Herrmann and Funes, 2005; Mick et al., 2011). Defects in cytochrome oxidase function, caused by mutations in structural subunits, inproper formation of the redox centers, or the lack of functional assembly factors, lead to severe neuromuscular disorders known as mitochondrial encephalomyopathies (DiMauro and Schon, 2003; Shoubridge, 2001; Zeviani and Spinazzola, 2003).

The crystal structure of the bovine cytochrome oxidase reveals a dimeric enzyme with COX6a (Cox13 in yeast) at the interface of the two monomers (Tsukihara et al., 1996). In the inner mitochondrial membrane, cytochrome oxidase does not act as a single entity but associates with other complexes of the respiratory chain into respirasomes, supercomplexes of several respiratory chain complexes (Althoff et al., 2011; Schägger and Pfeiffer, 2000; Stuart, 2008). This oligomerization enhances respiratory chain activity through spatial restriction of electron carrier diffusion (Acín-Pérez et al., 2008). In *Saccharomyces cerevisiae*, cytochrome oxidase associates with the bc_1-complex (complex III), forming two distinct complexes that can be separated by Blue native PAGE analyses, consisting of

a single complex IV associated to a dimer of complex III (III_2IV) or two complex IVs associated with a complex III dimer (III_2IV_2). Due to the presence of NADH dehydrogenase (complex I) in human mitochondria, the oligomerization pattern is more complex. Similarly, oligomerization has also been reported for the F_1F_oATPase of mitochondria (Arnold et al., 1998). Several specific dimerization factors have been identified that regulate the oligomerization of the F_1F_oATPase in a process that appears to be fine-tuned by the posttranslational modification of the assembly factor Atp20 (Reinders et al., 2007). While oligomerization appears to have little effect on the activity of the enzyme, oligomers of the F_1F_oATPase have been found to be important in inner mitochondrial membrane cristae organization (Paumard et al., 2002; Rabl et al., 2009; Wagner et al., 2009). In contrast to the F_1F_oATPase, no protein factors have thus far been identified that specifically regulate respiratory chain supercomplex formation. Thus, the role of supercomplex formation in mitochondria is still ill defined. However, cardiolipin, the hallmark phospholipid of mitochondria, is important to stabilize mitochondrial membrane protein complexes including respiratory chain supercomplexes (Pfeiffer et al., 2003; Zhang et al., 2002, 2005). Thus, yeast mitochondria defective in cardiolipin synthesis display supercomplex dissociation (Brandner et al., 2005). In Barth syndrome patients, in which cardiolipin remodeling is affected, a similar destabilization of supercomplexes is observed and believed to contribute to the pathology of the disorder (McKenzie et al., 2006).

Here we identified Rcf1 and Rcf2 as two structural subunits of the yeast cytochrome oxidase that interact with the bc_1 complex. While Rcf2 is conserved among yeast species, Rcf1 possesses eukaryotic homologs including two human variants (RCF1a and RCF1b). Yeast cells lacking Rcf1 are affected in cytochrome oxidase function and display increased production of reactive oxygen species (ROS). We find that Rcf1 is required for assembly of the structural subunits Cox13 and Rcf2 into cytochrome oxidase complexes. Moreover, Rcf1 is required for respirasome formation, and loss of Rcf1 causes the selective deficiency of supercomplexes consisting of a bc_1 complex dimer and two cytochrome oxidase complexes. Thus, Rcf1 is the first protein mediating respirasome formation. Moreover, identification of Rcf1 revealed that, in contrast to the established view, mitochondria possess at least two different enzymatically active cytochrome oxidase forms, which are distinguishable by their protein composition. Both forms of the complex are independently incorporated into respirasomes. Our analyses indicate that a Cox13-containing isoform, that is selectively deficient in *rcf1*Δ mitochondria, is required to protect the respiratory chain from malfunction and thus ROS generation under hypoxic conditions.

RESULTS

Identification of Rcf1 and Rcf2

In *S. cerevisiae*, complex III is found in a dimeric form and in complex with one or two copies of complex IV, while the F_1F_oATPase is found in a monomeric or a dimeric form, which can be separated and analyzed by Blue native PAGE (BN-PAGE) (Schägger and Pfeiffer, 2000; Stuart, 2008). However, the molecular composition of these complexes is still ill defined. In addition to respiratory chain complexes, a large number of diverse proteins have been found to associate with respiratory chain complexes within supercomplexes. Among these proteins are, e.g., assembly factors of the respiratory chain (Mick et al., 2007), translational regulators (Mick et al., 2010), mitochondrial metabolite carriers (Dienhart and Stuart, 2008), the presequence translocase (Saddar et al., 2008; van der Laan et al., 2006), subunits of the import motor (Wiedemann et al., 2007), lipid-modifying enzymes (Claypool et al., 2008), and fatty acid β oxidation enzymes (Wang et al., 2010). To identify supercomplex-associated factors that could fall into one of the different categories described above, we purified complex III/IV supercomplexes from digitonin-solubilized mitochondria by affinity chromatography using a TAP-tagged version of the complex III subunit Cor1 and a wild-type strain lacking a tag on Cor1 as a control (van der Laan et al., 2006; Wiedemann et al., 2007). As a second dimension of purification, we separated the isolated complexes by BN-PAGE (Figure 1A). Protein complexes were excised from the gel and subjected to in-gel digestion, and peptides were analyzed by mass spectrometry. As expected, we identified known structural subunits of complex III and complex IV as well as a number of the known associated factors (Table 1 and see Table S1 available online). However, we also identified two uncharacterized proteins that we later termed Rcf1 (YML030W) and Rcf2 (YNR018W) (Respiratory Supercomplex Factor 1/2). In a genome-wide screen for genes involved in mitochondrial inheritance, these genes had been identified as Aim31 and Aim38; however, a function had not yet been attributed (Hess et al., 2009). Moreover, a proteomic analysis of crude mitochondrial extracts separated by BN-PAGE had suggested comigration of these proteins with supercomplexes but addressed neither their function nor into which group of supercomplex-associated factors they could be assigned (Helbig et al., 2009). We confirmed the mass spectrometric result by western blot analyses of purified supercomplexes. Similar to the known structural subunits of the respiratory chain, Rcf1 and Rcf2 were copurified with $Cor1^{TAP}$ (Figure 1B). Rcf1 is a protein of 18 kDa with two predicted transmembrane helices. Similarly, Rcf2 consists of two predicted transmembrane helices and has a size of 25 kDa (Figure 1C). Both proteins lack an obvious N-terminal presequence for targeting into mitochondria. In agreement, when both proteins were synthesized in reticulocyte lysate and imported into isolated mitochondria, efficient in vitro import was observed; however, no processing to a faster-migrating mature form was seen (Figure S1A). Carbonate extraction analyses of isolated mitochondria showed that Rcf1 and Rcf2 were resistant to alkaline treatment and remained in the sediment together with integral membrane proteins, but both proteins were released upon membrane solubilization with Triton X-100 (Figure 1D). Antibodies against Rcf1 and Rcf2 were directed against C-terminal domains of the proteins. When mitochondria were treated with proteases, both proteins remained unaffected. However, the antigenic epitopes of Rcf1 and Rcf2 became accessible to protease treatment when the outer membrane was ruptured by osmotic swelling (mitoplast formation), and no faster-migrating proteolytic fragments were detected (Figure 1E and Figure S1B). We concluded that Rcf1 and Rcf2 are integral proteins of the mitochondrial inner membrane and expose their C termini to the intermembrane space.

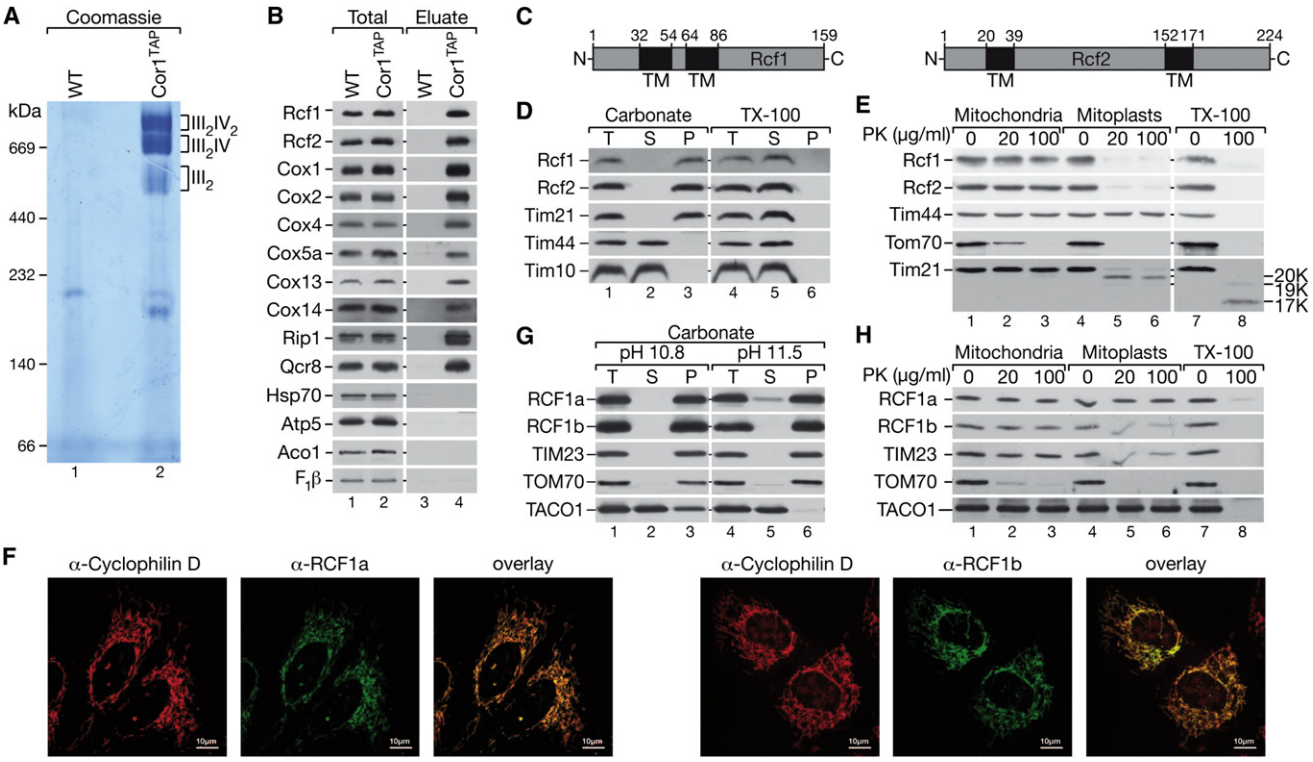

Figure 1. Purification of Respiratory Chain Supercomplexes and Identification of Rcf1 and Rcf2

(A) Mitochondria isolated from wild-type (WT), and *cor1*^{TAP} strains were solubilized in 1% digitonin and subjected to IgG chromatography. Upon TEV protease cleavage, eluates were analyzed by BN-PAGE and subjected to mass spectrometric analysis.

(B) Eluates from (A) were analyzed by SDS-PAGE, western blotting, and immunodecoration. Total, 10%; eluate, 100%.

(C) Schematic representation of Rcf1 and Rcf2 proteins. Black boxes, predicted transmembrane domains (TM); numbers indicate amino acids.

(D) Yeast mitochondria were subjected to carbonate extraction or lysed with 1% Triton X-100 followed by separation into pellet (P) and supernatant (S); total (T). Samples were subjected to western blot analysis.

(E) Yeast mitochondria were left untreated, swollen, or lysed with 1% Triton X-100; treated with Proteinase K where indicated; and subjected to SDS-PAGE and western blotting.

(F) Immunofluorescence analysis of U2-OS cells using cyclophilin D and RCF1a- and RCF1b-specific antibodies. Scale bar, 10 μm.

(G) HEK293 mitochondria were subjected to carbonate extraction. Pellet (P), supernatant (S), total (T).

(H) HEK293 mitochondria were treated as in (E). See also Figure S2.

While Rcf2 is conserved among yeast (Figure S2C), putative Rcf1 homologs were identified from yeast to plants, mouse, and human (Figures S2A–S2C). Two variants of Rcf1 could be identified in silico in human (RCF1a [Q9Y241-2] and RCF1b [Q9BW72]) and mouse. We assessed expression in different murine tissues by quantitative real-time PCR analyses and found that RCF1a and RCF1b were especially expressed in metabolically active tissues such as heart, liver, and kidney (Figure S1C). We next addressed the subcellular localization of RCF1a and RCF1b by immunofluorescence analysis and found both fully colocalized with mitochondrial cyclophilin D (Figure 1F). RCF1a and RCF1b were present in isolated human mitochondria and behaved as integral membrane proteins in carbonate extraction similar to TIM23 and TOM70, while the peripheral membrane protein TACO1 was released from membranes at pH 11.5 (Figure 1G). Protease protection experiments revealed that RCF1a and RCF1b remained protected in mitochondria. However, while RCF1b became accessible to protease treatment in mitoplasts, RCF1a was not affected by the treatment, and no stable degradation products were detected (Figure 1H and Figure S1D). Thus, human RCF1a and RCF1b are inner mitochondrial membrane proteins of which RCF1b displays topology similar to that of yeast Rcf1 and is partially exposed to the intermembrane space.

Rcf1 and Rcf2 Are Associated with Cytochrome Oxidase

Until this point, our analyses had yet to reveal if Rcf1 and Rcf2 were associated with complex III or complex IV. Therefore, we imported both proteins into isolated mitochondria. SDS-PAGE analyses showed that both proteins were efficiently transported into mitochondria in a membrane potential-dependent manner (Figure S1A). After import, mitochondria were reisolated, solubilized, and protein complexes separated by BN-PAGE. Rcf1 and Rcf2 assembled predominantly into two high molecular weight protein complexes. These complexes comigrated with respiratory chain supercomplexes consisting of complex III and IV (Figure 2A). This migration pattern was reminiscent of complex IV, as no complexes were apparent that corresponded in size to complex III dimers. The less abundant lower molecular weight complexes of Rcf1 and Rcf2 likely represent assembly

Table 1. Proteins of Respiratory Chain Supercomplexes Found by Cor1^{TAP} Affinity Purification

Subunits of Cytochrome *c* Reductase, bc_1	Subunits of Cytochrome *c* Oxidase, COX	Assembly Factors and Associated Proteins
COR1/YBL045C	COX1/Q0045	CBP3/YPL215W
QCR2/YPR191W	COX2/Q0250	CBP4/YGR174C
QCR6/YFR033C	COX3/Q0275[a]	SHY1/YGR112W
QCR7/YDR529C	COX4/YGL187C	COX11/YPL132W
QCR8/YJL166W	COX5a/YNL052W	COX14/YML129C
QCR9/YGR183C	COX5b/YIL111W	COX16/YJL003W
RIP1/YEL024W	COX6/YHR051W	TIM21/YGR033C
COB/Q0105	COX7/YMR256C	MDM38/YOL027C
CYT1/YOR065W	COX8/YLR395C	AAC2/YBL030C
	COX9/YDL067C	PET54/YGR222W
	COX12/YLR038C	
	COX13/YGL191W	
	COX26/YDR119W-A	
	RCF1/YML030W	
	RCF2/YNR018W	

[a] Detected only in BN-PAGE.

intermediates of the two imported proteins. To support complex IV association, we imported both proteins into mutant mitochondria. *cox4*Δ mitochondria lack mature complex IV, while *cyt1*Δ mitochondria are deficient in complex III. In *cox4*Δ mitochondria, complex III is found exclusively as a dimer, while in *cyt1*Δ mitochondria complex IV displayed as two complexes of different signal intensity between 230 and 440 kDa (Figure 2B, lanes 14 and 16). Rcf1 and Rcf2 were imported with similar efficiency into mutant mitochondria (Figure S1E). However, when assembled Rcf1 and Rcf2 were analyzed by BN-PAGE, they exhibited migration similar to Cox4 and Cox13 in *cyt1*Δ mitochondria but did not assemble into high molecular weight complexes in *cox4*Δ mitochondria (Figure 2B).

To address if human RCF1a and RCF1b were also genuine subunits of complex IV in human mitochondria, we first imported human RCF1b into isolated human mitochondria in vitro. The protein assembled in a membrane potential-dependent manner into a complex of approximately 450 kDa that comigrated with monomeric complex IV and RCF1a as visualized by western blotting (Figure 2C). Moreover, a fraction of RCF1a was also detected in respiratory chain supercomplexes in human mitochondria by western blotting. In addition, immunoprecipitation experiments using antibodies against holocomplex IV and the F_1F_o-ATPase as a control specifically copurified RCF1a and RCF1b with complex IV (Figure 2D). Thus, Rcf1 and Rcf2 are subunits of complex IV and supercomplexes in yeast. Similarly, RCF1a and RCF1b are constituents of human complex IV.

Loss of Rcf1 Affects Cytochrome Oxidase Function and Promotes ROS Generation

To assess the function of Rcf1 and Rcf2 in regards to respiratory chain activity, we generated gene deletion mutants. While Rcf1 and Rcf2 were dispensable for growth of yeast cells on fermentable carbon sources, *rcf1*Δ displayed growth defects on nonfermentable medium such as glycerol. In the course of analyses, we recognized that the growth phenotype of *rcf1*Δ cells was exacerbated when plates were grown under low-oxygen conditions (Figure 3A). This defect was less pronounced than that observed in a respiratory-deficient mutant such as *cox4*Δ (affected in a core subunit of the complex) but significantly more dramatic than that of *cox13*Δ cells (affected in a peripherally localized protein), which displayed growth behavior close to wild-type. In contrast to *rcf1*Δ cells, *rcf2*Δ and *rcf2*Δ/*cox13*Δ double mutant cells displayed growth behavior similar to that of *cox13*Δ cells (Figure 3A and Figure S3A). To support our conclusion that *rcf1*Δ cells were especially sensitive to hypoxia, we grew wild-type and *rcf1*Δ cells on fermentable carbon source in a fermentor under normoxic and hypoxic conditions. While both strains displayed similar division time under normoxia, *rcf1*Δ cells were severely affected under hypoxic growth conditions (Figure 3B).

We compared the steady-state protein levels of selected mitochondrial proteins between wild-type, *rcf1*Δ, and *rcf2*Δ by western blotting. Most proteins were similar in all three strains; however, the amount of Cox13 was dramatically reduced in *rcf1*Δ mitochondria (Figure 3C). In *cox13*Δ and *rcf2*Δ/*cox13*Δ mitochondria the levels of Rcf1 were not affected (Figures S3B and S3C). We assayed O_2 consumption in wild-type and mutant mitochondria with a Clark oxygen electrode. *rcf1*Δ mitochondria displayed drastically reduced oxygen consumption, similar to the defect observed upon loss of Cox13 (Figure 3D). In contrast, *rcf2*Δ mitochondria resembled wild-type mitochondria with regard to oxygen reduction, while *rcf2*Δ/*cox13*Δ double mutant mitochondria were similar to mitochondria from a *cox13*Δ mutant (Figure S3D). Enzyme activity assays demonstrated that *rcf1*Δ and *cox13*Δ cells were specifically defective in cytochrome oxidase activity, but *rcf2*Δ mitochondria were not affected (Figure 3E). Accordingly, Rcf1 is required for cytochrome oxidase activity to a similar extent as Cox13, but Rcf2 appears to be dispensable for its activity under the conditions used in this study. Interestingly, when we measured mitochondrial enzyme activities, we recognized a significant reduction in aconitase activity in *rcf1*Δ and *rcf2*Δ mitochondria (Figure 3F), even though the amount of aconitase (Aco1) was comparable to wild-type (Figure 3C). Since the 4Fe-4S cluster of aconitase is especially sensitive to superoxide (O_2^-) (for review, see Raha and Robinson, 2000), we addressed if the mutant mitochondria displayed overall increased ROS production using H_2DCFDA (dichlorodihydrofluorescein diacetate) that detects a broad range of different ROS. While *rcf1*Δ and *rcf2*Δ mitochondria displayed a drastic increase in ROS generation compared to wild-type mitochondria, *cox13*Δ mitochondria showed an intermediate phenotype (Figure 3G). In contrast, mitochondria that lacked Cox1, the heme-containing core subunit of complex IV, showed wild-type-like ROS generation (Figure S3E). Thus, Rcf1, Rcf2, and Cox13 appear to be uniquely important constituents of complex IV that protect mitochondria against ROS generation by the respiratory chain. Based on these findings, we asked if RCF1a and RCF1b were able to substitute for a lack of Rcf1 in yeast mitochondria. Expression of RCF1b but not RCF1a reproducibly improved the growth phenotype of

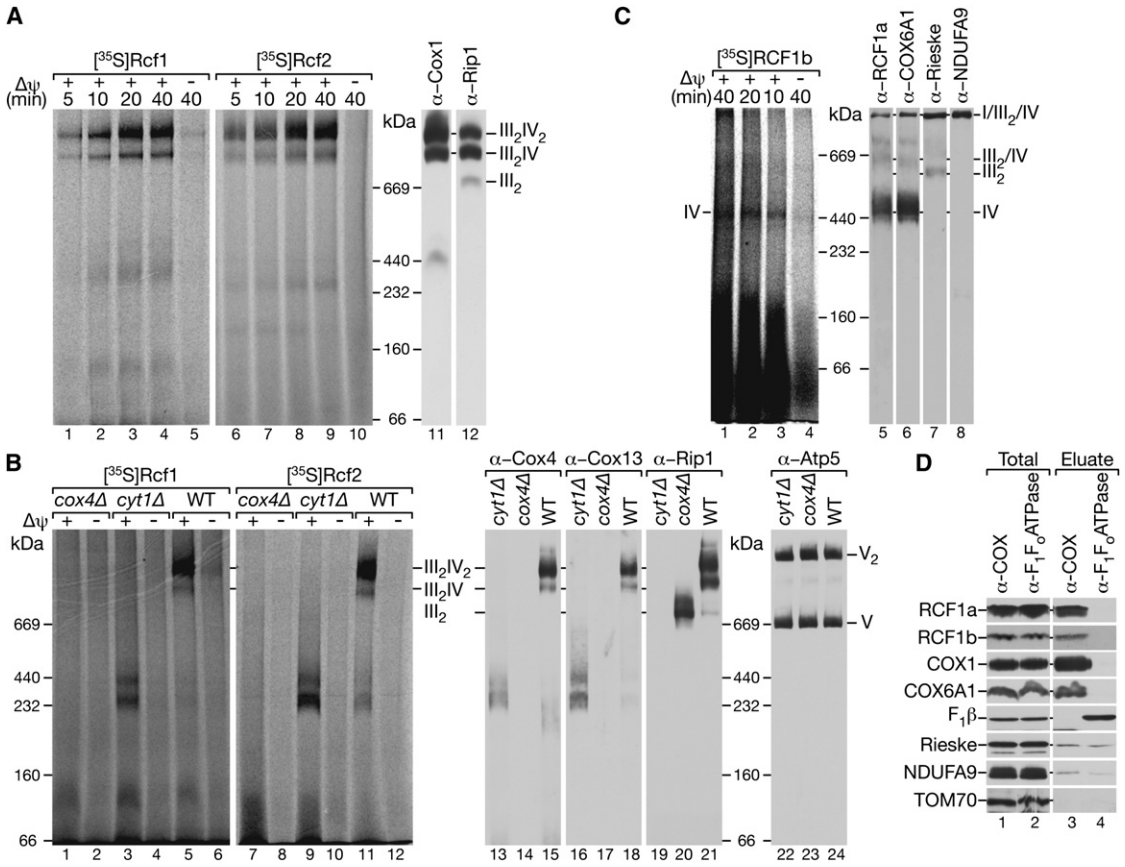

Figure 2. Rcf1 and Rcf2 Associate with Cytochrome Oxidase

(A) Radiolabeled Rcf1 and Rcf2 were imported into isolated yeast mitochondria in the presence or absence of membrane potential (Δψ) for indicated times. Samples were treated with Proteinase K, solubilized in 1% digitonin buffer, and analyzed by BN-PAGE and digital autoradiography. For comparison, solubilized mitochondria were analyzed by BN-PAGE, followed by western blotting and immunodecoration.

(B) Radiolabeled Rcf1 and Rcf2 were imported into isolated yeast mitochondria from WT, *cox4Δ*, and *cyt1Δ* cells and analyzed as in (A).

(C) Radiolabeled RCF1b was imported into mitochondria isolated from HEK293 cells, in the presence or absence of membrane potential (Δψ), treated with Proteinase K, solubilized in digitonin-buffer. Samples were analyzed by BN-PAGE and digital autoradiography. For comparison, mitochondria isolated from HEK293 cells were solubilized in digitonin and analyzed by BN-PAGE, followed by western blotting and immunodecoration.

(D) Coimmunoprecipitation of cytochrome oxidase (COX) and F_1F_oATPase from digitonin-solubilized mitochondria isolated from HEK293 cells. Total, 1.5%; elution, 100%. See also Figure S1.

*rcf1*Δ cells (Figure 3H). We noted that the yeast *RCF1* only partially complemented the growth defect of the deletion strain due to slightly reduced expression levels from the plasmid, suggesting that the amount of Rcf1 was rate limiting. Therefore, we analyzed complementation of *rcf1*Δ by human and yeast RCF1 with regard to ROS production under nonlimiting expression levels. Upon expression of Rcf1 and RCF1b in *rcf1*Δ, ROS production was drastically reduced, while expression of RCF1a had no effect on the mutant phenotype (Figure S4A). Thus, RCF1b is able to substitute Rcf1 functions in yeast mitochondria.

Assembly of Cox13 and Rcf2 Depends on Rcf1

Cox13 is a conserved structural subunit of complex IV, which localizes to the periphery of the complex in the crystal structure of bovine complex IV (Tsukihara et al., 1996). We speculated that the reduced amount of Cox13 observed in *rcf1*Δ mitochondria was due to an import or assembly defect. Therefore, we assayed assembly of Cox13, Rcf1, and Rcf2 in the different mutants. We synthesized and radiolabeled Cox13, Rcf1, and Rcf2 in reticulocyte lysate and performed in vitro import into wild-type, *cox13*Δ, *rcf1*Δ, and *rcf2*Δ mitochondria. After import, mitochondria were solubilized in digitonin buffer and complexes separated on BN-PAGE. Rcf2 efficiently assembled into supercomplexes in wild-type mitochondria, but assembly was blocked in the absence of Cox13 (Figure 4A, upper panel) or Rcf1 (Figure 4B, upper panel). To exclude the possibility that assembly defects were indirectly caused by a block of precursor import, we analyzed samples by SDS-PAGE and found that the import of Rcf2 was similar in mutant and wild-type mitochondria (Figures 4A and 4B, lower panels). Assembly of Cox13 into supercomplexes was similar to wild-type in *rcf2*Δ mitochondria (Figure 4C, upper panel) but completely blocked in *rcf1*Δ mitochondria (Figure 4D, upper panel). Again, import of Cox13 as assayed by SDS-PAGE, was unaffected in both mutants (Figures 4C and 4D, lower panels). Lastly, we analyzed import and assembly

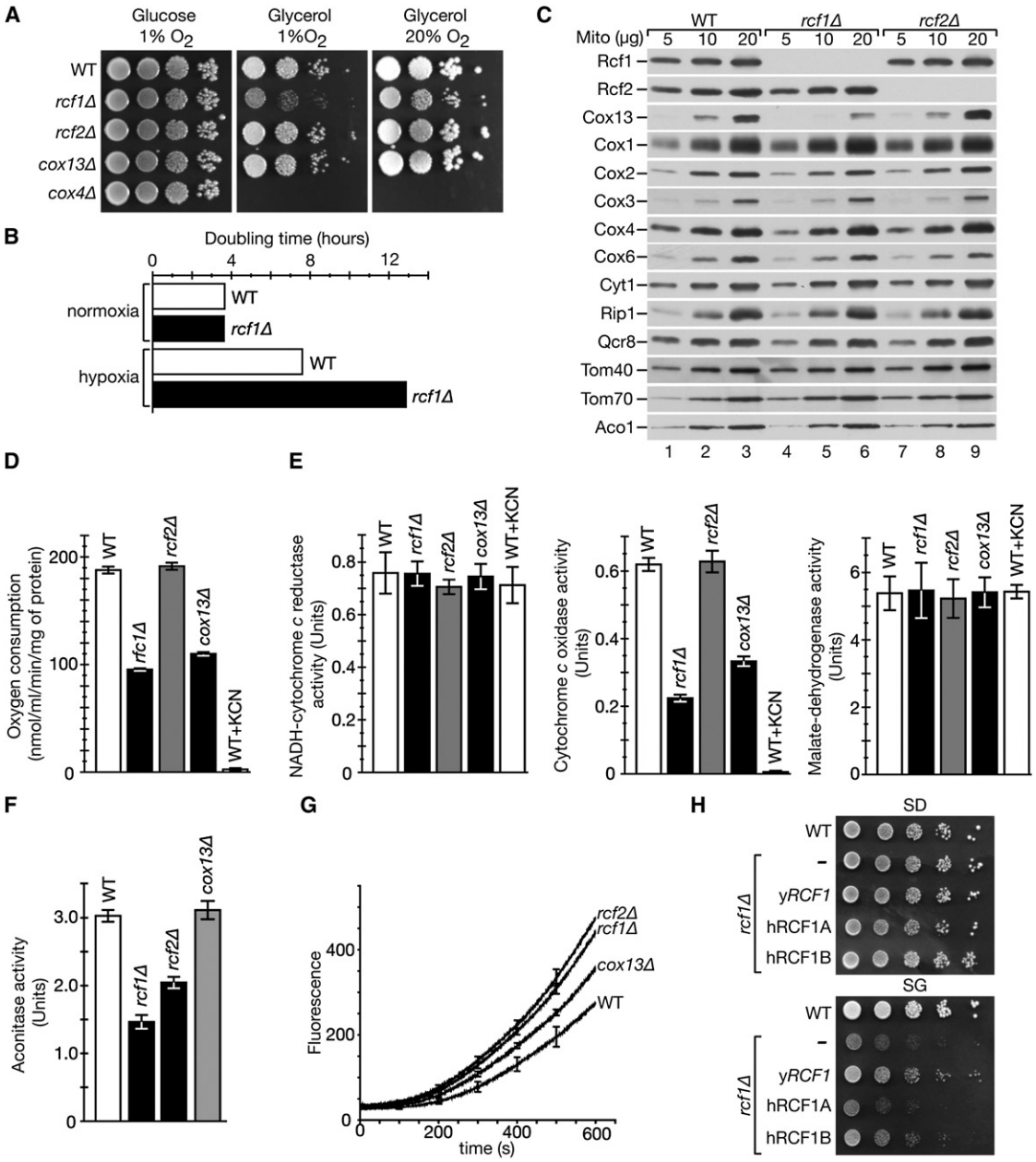

Figure 3. *rcf1Δ* Cells Have Reduced Respiratory Efficiency

(A) Growth test of wild-type (WT), *rcf1Δ*, *rcf2Δ*, *cox13Δ*, and *cox4Δ* yeast cells.

(B) Growth rate analysis of wild-type (WT) and *rcf1Δ* yeast cells in liquid medium.

(C) Isolated wild-type (WT), *rcf1Δ*, and *rcf2Δ* mitochondria were subjected to SDS-PAGE and analyzed by western blotting.

(D) Oxygen consumption measurements of mitochondria isolated from indicated strains.

(E) Mitochondrial enzyme assays of NADH-cytochrome *c* reductase, cytochrome *c* oxidase, and malate-dehydrogenase.

(F) Aconitase activities of isolated mitochondria.

(G) Mitochondrial ROS production in indicated strains. (D)–(G) Means of three independent measurements (SEM, n = 3).

(H) Complementation of yeast *rcf1Δ* on nonfermentable medium with yeast y*RCF1* gene and human hRCF1A and hRCF1B genes. SD, selective glucose; SG, selective glycerol. See also Figure S3.

of Rcf1 and found that both were unaffected in *cox13*Δ and *rcf1*Δ mitochondria (Figures 4E and 4F). In conclusion, we find that Rcf1 is required for efficient assembly of Cox13 and Rcf2 into supercomplexes. Furthermore, assembly of Rcf2 also depends on the presence of Cox13. Neither Cox13 nor Rcf1 assembly is Rcf2 dependent. These analyses suggest that the three proteins assemble in a successive manner with Rcf1 being first, followed by Cox13 and Rcf2.

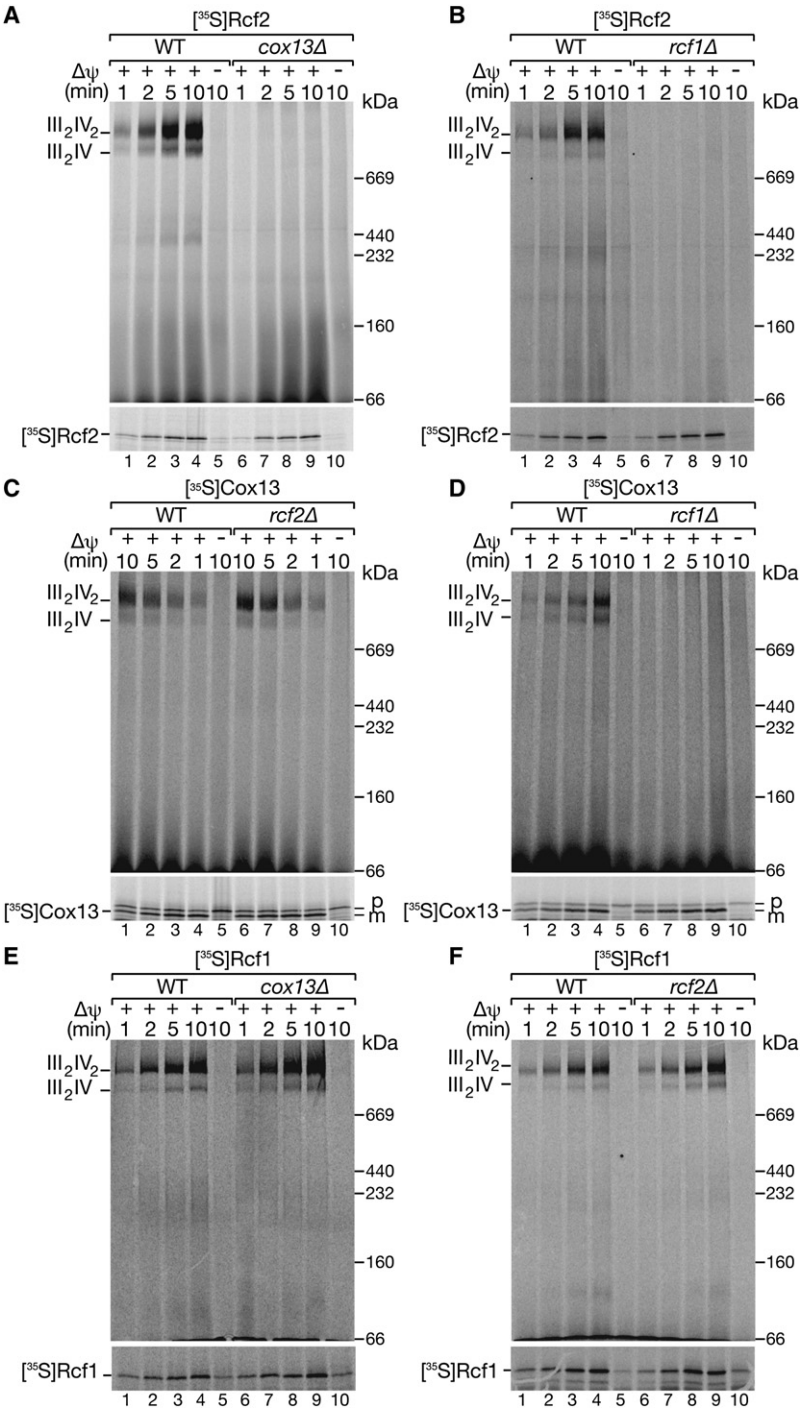

Figure 4. Assembly of Cox13 and Rcf2 into Cytochrome Oxidase Is Rcf1 Dependent

Radiolabeled Rcf2, Cox13, and Rcf1 were imported into isolated yeast mitochondria in the presence or absence of $\Delta\psi$ for indicated times and treated with Proteinase K. Samples were lysed in 1% digitonin buffer, analyzed by BN-PAGE or SDS-PAGE and digital autoradiography. Rcf2 was imported into WT/*cox13*Δ mitochondria (A) and WT/*rcf1*Δ mitochondria (B). Cox13 was imported into WT/*rcf2*Δ mitochondria (C) and WT/*rcf1*Δ mitochondria (D). Rcf1 was imported into WT/*cox13*Δ mitochondria (E) and WT/*rcf2*Δ mitochondria (F).

Rcf1 Is Required for Formation of Supercomplexes in Mitochondria

To address the organization of respiratory chain supercomplexes at steady state, we solubilized *cox13*Δ, *rcf1*Δ, and *rcf2*Δ mitochondria in digitonin-containing buffer and performed BN-PAGE analyses. All mutant mitochondria possessed respiratory chain complexes III and IV. However, *rcf1*Δ mitochondria displayed a dramatic loss of III_2IV_2 complexes compared to wild-type, *cox13*Δ, *rcf2*Δ, *cox13*Δ/*rcf2*Δ, and *taz1*Δ (involved in cardiolipin biosynthesis) mitochondria (Figure 5A; Figures S4B and S4C). While Cox13 and Rcf2 assembly was severely affected in *rcf1*Δ mitochondria (see above), at steady state a low amount of both proteins was present in respiratory chain complexes of *rcf1*Δ mitochondria (Figure 5A, lanes 18 and 22). This finding suggests that Rcf1 is important but not essential for Cox13 and Rcf2 assembly and that a small amount of Rcf2 and Cox13 can accumulate in the complex in vivo. In *cox13*Δ mitochondria, Rcf2 was not recovered in supercomplexes but accumulated in an unassembled, probably monomeric form that was apparent in the low molecular weight range of BN-PAGE (Figure 5A, lane 20). (The antibody against Rcf1 was unable to detect the protein in BN-PAGE analyses.) Most striking was the observation that Rcf1 was specifically required for formation of respiratory chain supercomplexes. The amount of III_2IV_2 was drastically reduced, and at the same time III_2IV and free complex III_2 accumulated (Figure 5A), suggesting that III_2IV_2 complexes dissociate in the absence of Rcf1 or are not formed efficiently. This phenotype was fully reversed by expression of Rcf1 in *rcf1Δ* cells, but not by expression of RCF1a or RCF1b (Figure S4D).

If Rcf1 was generally required for association of complex IV to complex III_2, one would expect full dissociation of supercomplexes into monomeric complex IV and dimeric complex III in mutant strains. Thus, we considered two explanations for the observed phenotype: (1) *rcf1*Δ mitochondria could simply possess less complex IV so that the equilibrium between supercomplexes is altered in favor of III_2IV formation; (2) complex IV monomers that associate with complex III dimers are not identical in their composition, and therefore only a subfraction of complexes is affected by a lack of Rcf1.

To experimentally address the existence of distinct forms of complex IV, we first generated Cox4, Rcf2, and Cox13 fusions with ZZ tags and expressed the fusions in yeast from the chromosomal locus. Purification of $Cox4^{ZZ}$, $Cox13^{ZZ}$, and $Rcf2^{ZZ}$ from digitonin-solubilized mitochondria was possible and led

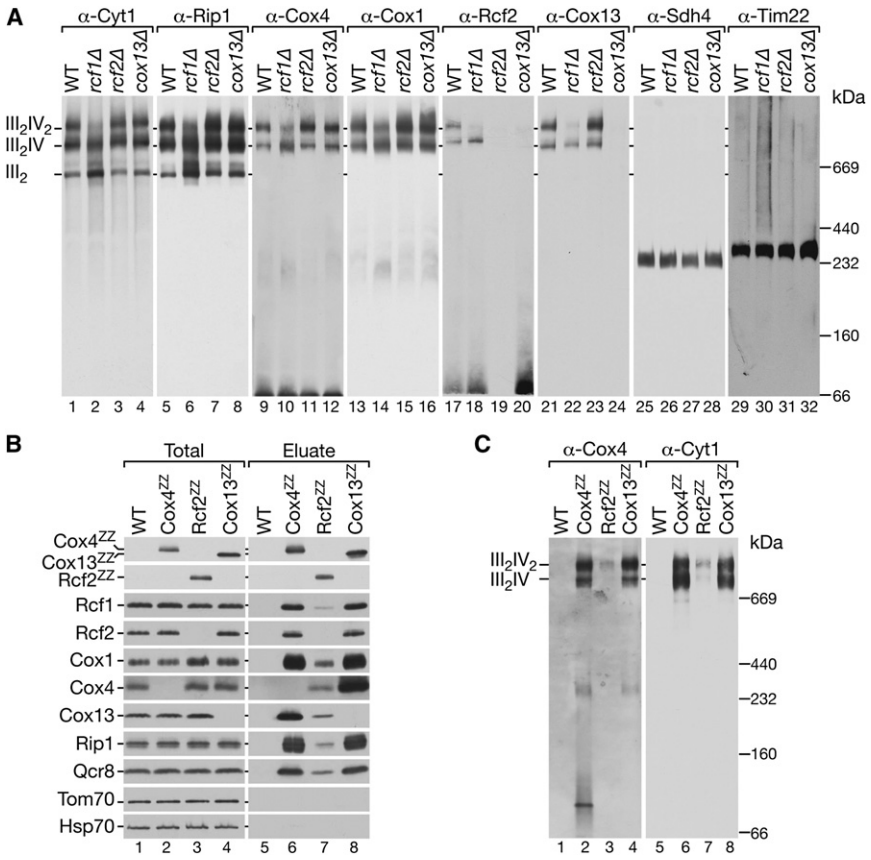

Figure 5. Formation of Respiratory Chain Supercomplexes Depends on Rcf1

(A) Mitochondria isolated from indicated strains were lysed in 1% digitonin buffer, subjected to BN-PAGE, and analyzed by western blotting.

(B) $Cox4^{ZZ}$, $Cox13^{ZZ}$, and $Rcf2^{ZZ}$ complexes were isolated from digitonin-solubilized mitochondria via IgG chromatography, analyzed by SDS-PAGE and western blotting. Total, 10%; eluate, 100%.

(C) Isolation of $Cox4^{ZZ}$, $Cox13^{ZZ}$, and $Rcf2^{ZZ}$ complexes was performed as in (B). Bound complexes were released from the column by TEV protease cleavage, analyzed by BN-PAGE and western blotting. Eluate fractions are presented. See also Figure S4.

to efficient coisolation of respiratory chain supercomplexes (Figure 5B). However, while $Cox4^{ZZ}$ and $Cox13^{ZZ}$ efficiently isolated complex IV and complex III, $Rcf2^{ZZ}$ was only associated with a fraction of supercomplexes under these conditions (Figure 5B, lane 7). This agreed with the BN-PAGE analyses in which a pool of Rcf2 migrated as a monomeric, unassembled form at the front of the gel (Figure 5A, lane 17). Moreover, when we purified $Cox4^{ZZ}$-, $Cox13^{ZZ}$-, and $Rcf2^{ZZ}$-containing complexes from digitonin-solubilized mitochondria and analyzed these by BN-PAGE, Rcf2 only copurified a small fraction of supercomplexes compared to Cox4 and Cox13 (Figure 5C). This finding indicates that Rcf2 is a substoichometric subunit of supercomplexes.

Distinct Forms of Cytochrome Oxidase Exist in Mitochondria

To dissociate supercomplexes into complex IV monomers and complex III dimers (Schägger and Pfeiffer, 2000), we solubilized mitochondria in dodecylmaltoside-containing buffer and isolated $Cox4^{ZZ}$- and $Cox13^{ZZ}$-containing complexes by IgG chromatography. In comparison to $Cox4^{ZZ}$ isolations, $Cox13^{ZZ}$ isolations copurified significantly fewer complex IV subunits. This became especially apparent upon comparison of the unbound fractions, which were depleted for complex IV subunits in $Cox4^{ZZ}$ isolations, but not in $Cox13^{ZZ}$ (Figure 6A). Rcf1 and Rcf2 dissociated from complex IV under these solubilization conditions. Only a fraction of Rcf1 (approximately 20%) could be detected in $Cox4^{ZZ}$-purification samples, while Rcf2 fully dissociated (Figure 6A). When we isolated complex III via Cor1 under these conditions, small amounts of Rcf1 and Rcf2 (approximately 5%) but not Cox13 or other subunits of complex IV copurified (Figure S4E). In summary, these analyses suggested that Cox13 was only associated with a subfraction of complex IV in mitochondria. Moreover, a fraction of Rcf1 and Rcf2 is associated with complex III, indicating that besides their preferential association with complex IV they can also interact with complex III. Thus, we hypothesize that Rcf1 and Rcf2 are likely to be present at the interface of complex III/IV oligomers.

Despite the fact that the steady-state protein analyses of *rcf1*Δ mitochondria had not indicated differences in the amounts of complex IV subunits compared to wild-type, with the exception of Cox13, we assessed directly the amount of complex IV and its organization in mutant mitochondria after solubilization in dodecylmaltoside-containing buffer. Solubilized complexes were separated by BN-PAGE and analyzed by western blotting. Cox1 was detected in distinct complexes of different size (termed IV and IV* here, Figure 6B). Depending on the resolution of the gel, IV* complexes migrated as one or two complexes. However, the number of IV* complexes was significantly fewer as compared to IV when an antibody against the core subunit Cox1 was used. In contrast to the core subunit Cox1, Cox13 was exclusively present in the slower-migrating IV* complexes (Figure 6B, lane 5). While complex IV levels were not significantly altered in *rcf1*Δ mitochondria, loss of Rcf1 caused a selective lack of the IV* forms, while the IV form remained largely unaffected. This defect was Rcf1 specific and not related to the absence of Cox13, since Cox1 was detected in IV and IV* complexes in *cox13Δ* mitochondria (Figure 6B). For comparison, we used NP-40 for solubilization and similarly observed two distinct forms of complex IV, of which only the larger one contained Cox13 (Figure 6C). The apparent migration differences of the complexes in the two detergents is likely due to differences in micellar size.

Our analyses did not rule out the possibility that the selective detection of Cox13 in the IV* complex was due to differential accessibility of the antigenic epitope in the two complexes.

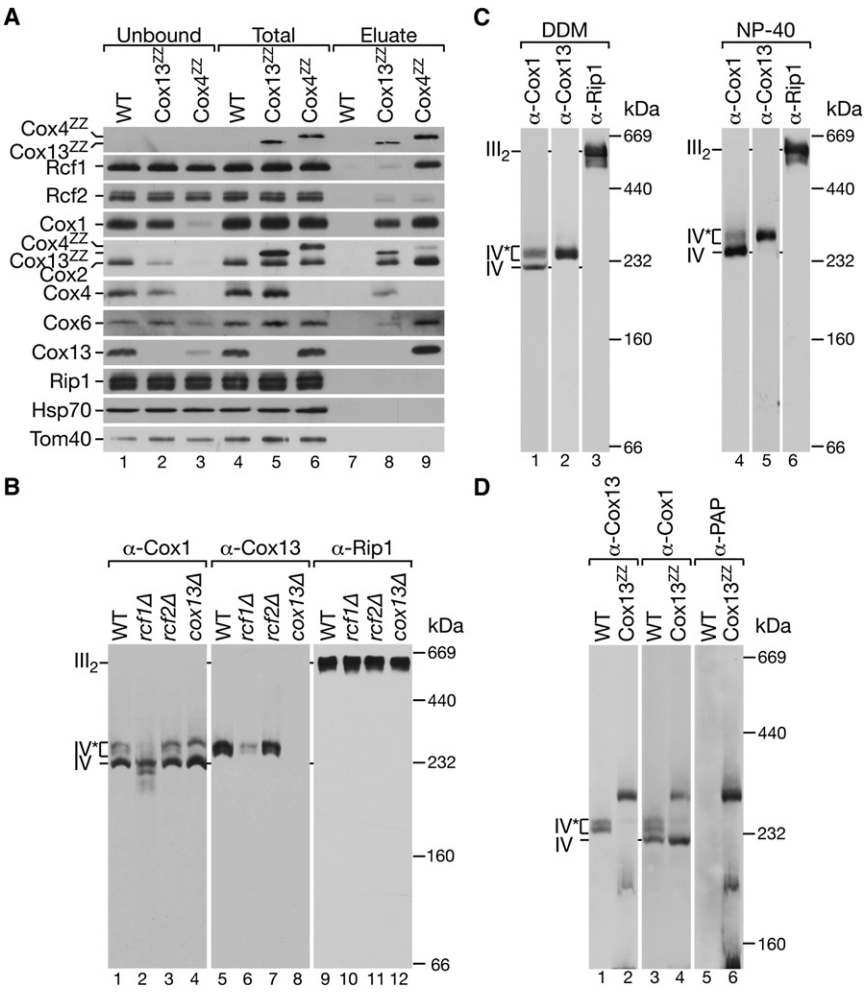

Figure 6. Complex IV Exists in Distinct Forms

(A) Cox4^{ZZ} and Cox13^{ZZ} complexes were isolated from DDM-solubilized mitochondria via IgG chromatography, analyzed by SDS-PAGE and western blotting. Total, unbound, 25%; elution, 100%.

(B) Mitochondria isolated from indicated strains were lysed in 0.6% DDM buffer, subjected to BN-PAGE, and analyzed by western blotting.

(C) Wild-type (WT) mitochondria were lysed in 0.6% DDM- or 0.5% NP-40-buffer, analyzed by BN-PAGE.

(D) Mitochondria isolated from wild-type (WT) and *cox13*^{ZZ} strains were solubilized in 0.6% DDM buffer, subjected to BN-PAGE and western blotting.

Therefore, we utilized the ZZ-tagged Cox13 to increase protein mass of the Cox13-containing complexes. After solubilization in DDM-containing buffer, complexes were analyzed by BN-PAGE. Compared to wild-type mitochondria, Cox13^{ZZ} mitochondria showed a specific mass shift of complex IV*, while complex IV remained unaltered (Figure 6D). This finding supports the conclusion that Cox13 is selectively present in complex IV*. Accordingly, Cox13 is a constituent of a defined subclass of cytochrome oxidase complexes in mitochondria. Rcf1 is specifically required for the formation of this complex isoform. We conclude that the lack of the Cox13-containing isoforms of complex IV in *rcf1*Δ mitochondria leads to the absence of the III_2IV_2 supercomplex.

DISCUSSION

The identification of respirasomes has changed our view on the organization of the respiratory chain and impacted the concept of electron shuttling between complexes (Acín-Pérez et al., 2008; Stuart, 2008; Wittig and Schägger, 2009). However, a mechanistic basis of supercomplex formation between respiratory chain complexes has remained undefined. While it is well documented that the lipid environment contributes to the stabilization of such supercomplexes, protein constituents required for the association between complexes have only been found in the case of the F_1F_o-ATPase (Arnold et al., 1998; Fontanesi et al., 2006; Pfeiffer et al., 2003; Zhang et al., 2002). However, a number of recent analyses have revealed that respiratory chain supercomplexes are in fact a yet-unresolved heterogeneous population of complexes in which a number of accessory factors can associate to respiratory chain oligomers (see above). This fact hampers the identification of specific oligomerization factors. Moreover, the lack of specific mutants that affect respiratory chain oligomerization represents an obstacle in addressing the physiological function of respirasomes in mitochondria.

Here we have identified Rcf1 and Rcf2 as two new subunits of the cytochrome oxidase. Rcf1 is a conserved protein with two variants in human mitochondria RCF1a and RCF1b. Upon expression in *rcf1*Δ mutant cells, RCF1b is able to alleviate growth defect and ROS production, indicating functional complementation. We show that Rcf1 is specifically required for supercomplex formation between cytochrome oxidase and bc_1 complexes in the inner membrane of mitochondria. Interestingly, a lack of Rcf1 does not affect all cytochrome oxidase complexes similarly, and a subset of complexes is still able to associate with bc_1 complexes in the absence of Rcf1. This phenotype is explained by the unexpected observation in which cytochrome oxidase exists in different forms that can be defined by the absence or presence of Cox13 (COX6a in human). Our analyses demonstrate that only a fraction of respiratory chain complexes contain Cox13, while the majority of cytochrome oxidase complexes are Cox13-free. Interestingly, the Cox13-containing form of the complex has been crystallized and displays a peripheral position of Cox13 (Tsukihara et al., 1996). Despite the fact that Rcf1 is a conserved constituent of the cytochrome oxidase complex, it was not identified in the X-ray structure. Our analyses show that complex association of Rcf1 and Rcf2 is affected by dodecylmaltoside treatment. Thus, it is

likely that proteins are lost from the complex under the purification conditions that have been used in previous analyses.

We show that Rcf1 is required for cytochrome oxidase activity and that lack of Rcf1 function leads to growth defects on nonfermentable carbon sources. The magnitude of the defect in cytochrome oxidase activity resembles that observed in mitochondria lacking Cox13. However, *rcf1*Δ cells display a more severe growth defect on nonfermentable carbon sources than do *cox13*Δ cells. Our analyses show that Rcf1 is specifically required for growth of yeast cells under hypoxic conditions. In contrast, Rcf2 is not required for cytochrome oxidase activity, at least not under the conditions used here. A clear Cox13 (COX6a) function has so far not been assigned, but the protein has been implicated in an ATP-dependent modulation of enzyme activity (Taanman and Capaldi, 1993). Interestingly, human COX6a displays tissue specificity and thus might be important for the fine-tuning of the complex with regard to the specific demands of the tissue (Fontanesi et al., 2008; Vijayasarathy et al., 1998). In line with the observed defects in cytochrome oxidase activity, we find that Rcf1 is required for efficient assembly of Cox13 and Rcf2, and that Cox13 is required for Rcf2 biogenesis, in contrast to Rcf1. Thus, the defect in cytochrome oxidase activity in *rcf1*Δ mitochondria is likely coupled to Cox13 function.

While Rcf2 deficiency did not cause an appreciable defect in the organization or activity of cytochrome oxidase in our analyses, we detected a significant increase in the production of ROS in *rcf2*Δ mitochondria. The same extent of ROS generation was measured in *rcf1*Δ mitochondria, while *cox13*Δ mitochondria displayed an intermediate phenotype as compared to wild-type. ROS production did not correlate with the defects in cytochrome oxidase activity, since this was not affected in *rcf2*Δ mitochondria and ROS production was not increased in *cox1*$^{-}$ mitochondria or in other tested *cox* mutant mitochondria. Moreover, the ROS phenotype also does not explain the selective growth defects seen for the mutants, since only *rcf1Δ* cells showed a growth defect under hypoxic conditions. How can these observations be reconciled with the fact that Cox13 marks a specific form of cytochrome oxidase and that Rcf1 but not Rcf2 is required for the formation of this complex? If one takes into consideration the observed dependencies of Cox13, Rcf1, and Rcf2 with regard to their assembly, it is likely that these proteins are present in the same cytochrome oxidase complexes. Unfortunately, Rcf2 fully dissociates from the IV* complex under conditions in which the complex can be dissected. Moreover, only small amounts of Rcf1 remain associated with Cox13 under these conditions (Figure 5C, lane 8). Therefore, only circumstantial evidence exists that these three proteins are constituents of the same complex. The fact that a fraction of Rcf1 and Rcf2, but not Cox13, remains associated with complex III when supercomplexes are dissociated by dodecylmaltoside suggests that these two proteins localize to the interface between complexes III and IV and are able to contact both. Considering the phenotype of *rcf1Δ*, it is tempting to speculate that Rcf1 could act as a physical link between complexes. However, the dramatic loss of III_2/IV_2 supercomplexes in *rcf1Δ* mitochondria cannot just be reconciled with the loss of complex IV*, since this complex represents the less abundant form of complex IV. However, it is conceivable that Rcf1 is not solely required to associate the IV* complex with complex III but could also act in associating the IV complex with complex III.

The presence of a specific isoform of complex IV, termed IV*, was an unexpected observation. As this complex is absent in *rcf1Δ* mitochondria and likely to contain Rcf2 and Cox13, we propose that the IV* complex serves to protect the respiratory chain from ROS generation and that a lack of any of the three proteins leads to malfunction and thus ROS production, probably in a catalytic manner. To confirm this model it will be important to further dissect the composition of the IV* complex and to devise a strategy to preserve accessibility to biochemical analyses in the future.

EXPERIMENTAL PROCEDURES

Protein Complex Isolation and Depletion Assay

Mitochondria containing TAP- or protein A-tagged proteins (10 mg for preparative scale, 1 mg or 0.5 mg for analytical scale, and 0.2 mg for depletion assay) were solubilized at 4°C in soulubilization buffer (100 mM NaCl, 20 mM Tris/HCl [pH 7.4], 5% [v/v] glycerol, 0.5 mM EDTA, 1% [w/v] digitonin, or 0.6% [w/v] DDM). After clarifying-spin samples were incubated with IgG Sepharose. Upon extensive washing with solubilization buffer containing 0.3% (w/v) digitonin or 0.2% (w/v) DDM, bound proteins were eluted by TEV protease cleavage or with SDS sample buffer, without β-mercaptoethanol to prevent release of IgG chains from the Sepharose, and subsequently analyzed by BN-PAGE or SDS-PAGE, western blotting, and mass spectrometry.

Immunoprecipitation

Immunoprecipitation of human mitochondrial complexes was performed either with beads coupled with anti-Complex IV antibodies or anti-Complex V antibodies (Invitrogen). Isolated mitochondria (1 mg) from HEK293T cells were solubilized at 4 C° in IP buffer (20 mM Tris [pH 7.4], 50 mM NaCl, 0.5 mM EDTA, 10% [w/v] glycerol, 1% [w/v] digitonin, 1 mM PMSF). After a clarifying spin, samples were incubated with the individual antibody-coupled beads for 1 hr at 4°C. Samples were washed ten times with W buffer (IP buffer with 0.3% [w/v] digitonin, 1 mM PMSF). Bound proteins were eluted with SDS sample buffer.

Protein Localization Analysis

Isolated mitochondria were converted to mitoplasts by hypotonic swelling in EM buffer (1 mM EDTA, 10 mM MOPS [pH 7.2]) or lysed in 1% Triton X-100 and then treated with Proteinase K. Mitochondria were subjected to extraction in 0.1 M Na_2CO_3 (pH 11.5 or pH 10.8), or 1% Triton X-100 supplemented with 150 mM NaCl, and then centrifuged at 45,000 rpm at 4°C for 45 min. Samples were precipitated with TCA and analyzed by SDS-PAGE and western blotting.

Immunofluorescence Assay

Immunofluorescence assay was performed according to Wurm et al. (2010). In brief, bone marrow U2-OS cells were grown on coverslips, fixed by incubation of coverslips for 5–10 min in 8% paraformaldehyde (PFA), and permeabilized by incubation in 0.5% (v/v) Triton X-100 for 5 min. Rabbit antisera against RCF1a (N-terminal peptide; Santa Cruz Biotech.) and RCF1b (whole protein) and mouse antisera against cyclophilin D were used at dilution 1:400. For detection, Alexa Fluor 488 conjugated goat anti-rabbit IgG and Alexa Fluor 594 conjugated goat anti-mouse IgG (Invitrogen) were used in dilution 1:500. Images were prepared using a microscope. Fluorescence microscopy was performed with a beam-scanning confocal microscope (TCS SP5, Leica Microsystems CMS GmbH, Wetzlar, Germany) equipped with 1.4 NA oil immersion lenses (100×; HCX PL APO, Leica). The confocal pinhole was set to 1 airy unit. Dual color images were obtained by sequential scanning. The images are maximum projections of z stacks. Except for contrast stretching, no image processing was applied.

In Vitro Import into Mitochondria

Mitochondrial precursor proteins were synthesized in rabbit reticulocyte lysate (Promega) in the presence of [^{35}S] methionine. Mitochondria were incubated

with precursor proteins in import buffer (Ryan et al., 2001) in the presence of 2 mM ATP, 2 mM NADH, and ATP-regeneration system (5 mM creatine phosphate and 0.1 mg/ml creatine kinase). The import reaction was stopped on ice by dissipation of $\Delta\psi$ with 8 μM antimycin A, 1 μM valinomycin, and 10 μM oligomycin. For assembly assays, mitochondria were lysed in 1% digitonin buffer and processed for BN-PAGE.

BN-PAGE Electrophoresis

Mitochondria were solubilized in buffer (20 mM Tris-HCl [pH 7.4], 0.1 mM EDTA, 50 mM NaCl, 10% [v/v] glycerol, and 1 mM PMSF) containing digitonin (1% [w/v]), DDM (0.6% [w/v] DDM), or NP-40 (0.5% [v/v] NP-40) and incubated for 15 min at 4°C. Following a clarifying spin at 16,000 × *g* for 10 min at 4°C, supernatants were mixed with 10× Blue native sample buffer (100 mM Bis-Tris [pH 7.0], 5% [w/v] Coomassie Brilliant Blue G-250, and 500 mM amino *n*-caproic acid). Polyacrylamide blue native gradient gels (4%–10%, 4%–13%, or 6%–10%) were used.

Miscellaneous

Standard techniques were used for SDS-PAGE and western blotting to PVDF membranes. Visualization of antibody-protein complexes was achieved by enhanced chemiluminescence (GE Healthcare). All protocols regarding mouse organ explantations were approved by the Niedersächsische Landesamt für Verbraucherschutz und Lebensmittelsicherheit (T11/07) and conform with the Directive 2010/63/EU of the European Parliament.

SUPPLEMENTAL INFORMATION

Supplemental Information includes four figures, one table, Supplemental Experimental Procedures, and Supplemental References and can be found with this article online at doi:10.1016/j.cmet.2012.01.016.

ACKNOWLEDGMENTS

We thank Drs. D. Görlich, G. Braus, and D.U. Mick for helpful discussion. We are indebted to J. Melin for critical reading of the manuscript and to Fabian Ludewig, Nadine Stoepel, and Magdalena Pawlas for technical assistance. This work was supported by the Deutsche Forschungsgemeinschaft, the Forschungsförderungsprogramm of the Medical School of the University of Göttingen to M.D., Excellence Initiative of the German Federal and State, Governments (EXC 294 BIOSS), the Ministerium für Innovation, Wissenschaft, Forschung und Technologie des Landes Nordrhein-Westfalen, and the Max-Planck-Society (P.R. and S.J.).

Received: September 26, 2011
Revised: December 23, 2011
Accepted: January 26, 2012
Published online: February 16, 2012

REFERENCES

Acín-Pérez, R., Fernández-Silva, P., Peleato, M.L., Pérez-Martos, A., and Enriquez, J.A. (2008). Respiratory active mitochondrial supercomplexes. Mol. Cell *32*, 529–539.

Althoff, T., Mills, D.J., Popot, J.-L., and Kühlbrandt, W. (2011). Arrangement of electron transport chain components in bovine mitochondrial supercomplex I(1)III(2)IV(1). EMBO J. *30*, 4652–4664.

Arnold, I., Pfeiffer, K., Neupert, W., Stuart, R., and Schägger, H. (1998). Yeast mitochondrial F1Fo-ATP synthase exists as a dimer: identification of three dimer-specific subunits. EMBO J. *17*, 7170–7178.

Brandner, K., Mick, D., Frazier, A., Taylor, R., Meisinger, C., and Rehling, P. (2005). Taz1, an outer mitochondrial membrane protein, affects stability and assembly of inner membrane protein complexes: implications for Barth syndrome. Mol. Biol. Cell *16*, 5202–5214.

Carr, H., and Winge, D. (2003). Assembly of cytochrome c oxidase within the mitochondrion. Acc. Chem. Res. *36*, 309–316.

Claypool, S.M., Boontheung, P., McCaffery, J.M., Loo, J.A., and Koehler, C.M. (2008). The cardiolipin transacylase, tafazzin, associates with two distinct respiratory components providing insight into Barth syndrome. Mol. Biol. Cell *19*, 5143–5155.

Dienhart, M., and Stuart, R. (2008). The yeast Aac2 protein exists in physical association with the cytochrome bc_1-COX supercomplex and the TIM23 machinery. Mol. Biol. Cell *19*, 3934–3943.

DiMauro, S., and Schon, E. (2003). Mitochondrial respiratory-chain diseases. N. Engl. J. Med. *348*, 2656–2668.

Fontanesi, F., Soto, I., Horn, D., and Barrientos, A. (2006). Assembly of mitochondrial cytochrome c-oxidase, a complicated and highly regulated cellular process. Am. J. Physiol. Cell Physiol. *291*, C1129–C1147.

Fontanesi, F., Soto, I., and Barrientos, A. (2008). Cytochrome c oxidase biogenesis: new levels of regulation. IUBMB Life *60*, 557–568.

Helbig, A.O., de Groot, M.J.L., van Gestel, R.A., Mohammed, S., de Hulster, E.A.F., Luttik, M.A.H., Daran-Lapujade, P., Pronk, J.T., Heck, A.J.R., and Slijper, M. (2009). A three-way proteomics strategy allows differential analysis of yeast mitochondrial membrane protein complexes under anaerobic and aerobic conditions. Proteomics *9*, 4787–4798.

Herrmann, J., and Funes, S. (2005). Biogenesis of cytochrome oxidase—sophisticated assembly lines in the mitochondrial inner membrane. Gene *354*, 43–52.

Hess, D.C., Myers, C.L., Huttenhower, C., Hibbs, M.A., Hayes, A.P., Paw, J., Clore, J.J., Mendoza, R.M., Luis, B.S., Nislow, C., et al. (2009). Computationally driven, quantitative experiments discover genes required for mitochondrial biogenesis. PLoS Genet. *5*, e1000407. 10.1371/journal.pgen.1000407.

McKenzie, M., Lazarou, M., Thorburn, D.R., and Ryan, M.T. (2006). Mitochondrial respiratory chain supercomplexes are destabilized in Barth syndrome patients. J. Mol. Biol. *361*, 462–469.

Mick, D., Wagner, K., van der Laan, M., Frazier, A., Perschil, I., Pawlas, M., Meyer, H., Warscheid, B., and Rehling, P. (2007). Shy1 couples Cox1 translational regulation to cytochrome c oxidase assembly. EMBO J. *26*, 4347–4358.

Mick, D.U., Vukotic, M., Piechura, H., Meyer, H.E., Warscheid, B., Deckers, M., and Rehling, P. (2010). Coa3 and Cox14 are essential for negative feedback regulation of *COX1* translation in mitochondria. J. Cell Biol. *191*, 141–154.

Mick, D.U., Fox, T.D., and Rehling, P. (2011). Inventory control: cytochrome c oxidase assembly regulates mitochondrial translation. Nat. Rev. Mol. Cell Biol. *12*, 14–20.

Paumard, P., Vaillier, J., Coulary, B., Schaeffer, J., Soubannier, V., Mueller, D.M., Brèthes, D., di Rago, J.-P., and Velours, J. (2002). The ATP synthase is involved in generating mitochondrial cristae morphology. EMBO J. *21*, 221–230.

Pfeiffer, K., Gohil, V., Stuart, R., Hunte, C., Brandt, U., Greenberg, M., and Schägger, H. (2003). Cardiolipin stabilizes respiratory chain supercomplexes. J. Biol. Chem. *278*, 52873–52880.

Rabl, R., Soubannier, V., Scholz, R., Vogel, F., Mendl, N., Vasiljev-Neumeyer, A., Körner, C., Jagasia, R., Keil, T., Baumeister, W., et al. (2009). Formation of cristae and crista junctions in mitochondria depends on antagonism between Fcj1 and Su e/g. J. Cell Biol. *185*, 1047–1063.

Raha, S., and Robinson, B.H. (2000). Mitochondria, oxygen free radicals, disease and aging. Trends Biochem. Sci. *25*, 502–508.

Reinders, J., Wagner, K., Zahedi, R., Stojanovski, D., Eyrich, B., van der Laan, M., Rehling, P., Sickmann, A., Pfanner, N., and Meisinger, C. (2007). Profiling phosphoproteins of yeast mitochondria reveals a role of phosphorylation in assembly of the ATP synthase. Mol. Cell. Proteomics *6*, 1896–1906.

Ryan, M., Voos, W., and Pfanner, N. (2001). Assaying protein import into mitochondria. Methods Cell Biol. *65*, 189–215.

Saddar, S., Dienhart, M., and Stuart, R. (2008). The F_1F_0-ATP synthase complex influences the assembly state of the cytochrome bc_1-cytochrome oxidase supercomplex and its association with the TIM23 machinery. J. Biol. Chem. *283*, 6677–6686.

Saraste, M. (1999). Oxidative phosphorylation at the fin de siecle. Science *283*, 1488–1493.

Schägger, H., and Pfeiffer, K. (2000). Supercomplexes in the respiratory chains of yeast and mammalian mitochondria. EMBO J. *19*, 1777–1783.

Shoubridge, E. (2001). Cytochrome c oxidase deficiency. Am. J. Med. Genet. *106*, 46–52.

Stuart, R.A. (2008). Supercomplex organization of the oxidative phosphorylation enzymes in yeast mitochondria. J. Bioenerg. Biomembr. *40*, 411–417.

Taanman, J., and Capaldi, R. (1993). Subunit VIa of yeast cytochrome c oxidase is not necessary for assembly of the enzyme complex but modulates the enzyme activity. Isolation and characterization of the nuclear-coded gene. J. Biol. Chem. *268*, 18754–18761.

Tsukihara, T., Aoyama, H., Yamashita, E., Tomizaki, T., Yamaguchi, H., Shinzawa-Itoh, K., Nakashima, R., Yaono, R., and Yoshikawa, S. (1996). The whole structure of the 13-subunit oxidized cytochrome c oxidase at 2.8 Å. Science *272*, 1136–1144.

van der Laan, M., Wiedemann, N., Mick, D., Guiard, B., Rehling, P., and Pfanner, N. (2006). A role for Tim21 in membrane-potential-dependent preprotein sorting in mitochondria. Curr. Biol. *16*, 2271–2276.

Vijayasarathy, C., Biunno, I., Lenka, N., Yang, M., Basu, A., Hall, I.P., and Avadhani, N.G. (1998). Variations in the subunit content and catalytic activity of the cytochrome c oxidase complex from different tissues and different cardiac compartments. Biochim. Biophys. Acta *1371*, 71–82.

Wagner, K., Rehling, P., Sanjuán Szklarz, L.K., Taylor, R.D., Pfanner, N., and van der Laan, M. (2009). Mitochondrial F_1F_o-ATP synthase: the small subunits e and g associate with monomeric complexes to trigger dimerization. J. Mol. Biol. *392*, 855–861.

Wang, Y., Mohsen, A.-W., Mihalik, S.J., Goetzman, E.S., and Vockley, J. (2010). Evidence for physical association of mitochondrial fatty acid oxidation and oxidative phosphorylation complexes. J. Biol. Chem. *285*, 29834–29841.

Wiedemann, N., van der Laan, M., Hutu, D.P., Rehling, P., and Pfanner, N. (2007). Sorting switch of mitochondrial presequence translocase involves coupling of motor module to respiratory chain. J. Cell Biol. *179*, 1115–1122.

Wittig, I., and Schägger, H. (2009). Supramolecular organization of ATP synthase and respiratory chain in mitochondrial membranes. Biochim. Biophys. Acta *1787*, 672–680.

Wurm, C.A., Suppanz, I.E., Stoldt, S., and Jakob, S. (2010). Rapid FlAsH labelling in the budding yeast Saccharomyces cerevisiae. J. Microsc. *240*, 6–13.

Yoshikawa, S., Muramoto, K., and Shinzawa-Itoh, K. (2011). Proton-pumping mechanism of cytochrome c oxidase. Annu. Rev. Biophys. *40*, 205–223.

Zeviani, M., and Spinazzola, A. (2003). Mitochondrial disorders. Curr. Neurol. Neurosci. Rep. *3*, 423–432.

Zhang, M., Mileykovskaya, E., and Dowhan, W. (2002). Gluing the respiratory chain together. J. Biol. Chem. *277*, 43553–43556.

Zhang, M., Mileykovskaya, E., and Dowhan, W. (2005). Cardiolipin is essential for organization of complexes III and IV into a supercomplex in intact yeast mitochondria. J. Biol. Chem. *280*, 29403–29408.